ORIGINAL PAPER

JMS Journal of Medical Science

The natural HLA-Peptidome of Sezary Syndrome: uncovering antigens for T cell-based immunotherapy

Lydon Nyambura

Department of Dermatology, Venerology and Allergology, Charité – Universitätsmedizin Berlin corporate member of Freie Universität Berlin, Humboldt-Universität zu Berlin, and Berlin Institute of Health, Berlin, Germany

https://orcid.org/0000-0003-2197-6048

Corresponding author: nodyl_w@yahoo.com

Kathrin Textoris-Taube

Core Facility – High-Throughput Mass Spectrometry, Charité – Universitätsmedizin Berlin, Corporate Member of Freie Universität Berlin and Humboldt-Universität zu Berlin, Core Facility – High-Throughput Mass Spectrometry, Berlin, Germany

https://orcid.org/0000-0002-1224-8236

Peter Walden

Department of Dermatology, Venerology and Allergology, Charité – Universitätsmedizin Berlin corporate member of Freie Universität Berlin, Humboldt-Universität zu Berlin, and Berlin Institute of Health, Berlin, Germany

https://orcid.org/0000-0002-8986-3667

https://doi.org/10.20883/medical.e1335

Keywords: Sezary syndrome, HLA-I peptides, LC-MS/MS, immunopeptidome, immunogenicity

Received 2025-07-03
Accepted 2025-09-17
Published 2025-09-30

How to Cite: Nyambura L, Textoris-Taube K, Walden P. The natural HLA-Peptidome of Sezary Syndrome: uncovering antigens for T cell-based immunotherapy. Journal of Medical Science. 2025 September;94(3);e1335. https://doi.org/10.20883/medical.e1335

ABSTRACT

Introduction. Sezary syndrome (SS) is a rare and aggressive form of cutaneous T-cell lymphoma that has a poor prognosis, with a median overall survival time of less than 3 years. Despite advances in its treatment, SS is a challenge to manage, often characterised by high rates of relapse and limited response to therapy in many patients. The main challenge for treatment, including vaccine development, is its heterogeneity in its molecular and genetic characteristics, clinical presentation, disease progression, and treatment response. Understanding the SS heterogeneity at the omics level is vital in developing T-cell-mediated immunotherapeutic.

Material and methods. In this study, naturally presented human leukocyte antigen class I (HLA-I) peptides were isolated from leukapheresis samples of SS patients and analysed using high-performance liquid chromatography coupled to tandem mass spectrometry (LC-MS/MS). The source proteins were evaluated for potential immunotherapy applications.

Results. The total number of HLA-I–restricted peptides and source proteins identified in SS leukapheresis patient samples was approximately the same, and they were heterogeneous and individualised. Only a small fraction of HLA-I peptides and source proteins was found to be shared between and among the patients. Peptide lengths were dominated by nanopeptides, with a preference for processing by chymotrypsin. The source proteins were predominantly from the cytoplasm and were primarily involved in biosynthesis and regulation. Furthermore, the HLA-I peptides were presented from proteins of the top 20 genes with somatic mutations in SS, which include *NCOR1, TRRAP, JAK3, PLCG1, TP53, and STAT3* (SS-associated antigens - SAAs). These SAAs had varying mutation types and frequencies, dominated by missense variants, with

allele-dependent immunogenicity being highest in HLA-A*11:01 and HLA-A*02:01, lowest for HLA-A*01:01. TRRAP showed high-affinity peptides and low gene expression levels in normal tissue (except *for STAT3*), as well as a significant protein interaction network, including JAK3 and STAT3 at the primary level.
Conclusions. This study's findings contribute to the overall understanding of the SS HLA-I peptidome landscape and highlight potential T-cell-mediated immunotherapeutic targets.

Introduction

Sezary syndrome (SS) is a rare and aggressive form of cutaneous T-cell lymphoma, characterised by the proliferation and accumulation of malignant T cells in the skin [1,2]. SS typically presents with generalised erythroderma, intense pruritus, and the presence of atypical Sezary cells in the peripheral blood [2]. The disease primarily affects older individuals, with a higher incidence in males [3]. Unfortunately, SS has a poor prognosis, with a median overall survival time of less than 3 years [3,4]. Therapeutic management of SS involves a multimodal approach, combining skin-directed therapies (topical corticosteroids, phototherapy, and local radiotherapy), extracorporeal photopheresis, systemic treatments such as retinoids, chemotherapy, and targeted agents [5–7]. Immunotherapies, including immune checkpoint inhibitors and adoptive T-cell therapy, show promise in enhancing anti-tumour immune responses [8]. Despite these advances in treatment, SS remains challenging to manage, often characterised by high rates of relapse and limited response to therapy in many patients [9].

The main challenge for SS treatment, including vaccine development, is its heterogeneity [7,10–12] in clinical presentation, disease progression, and treatment response, as well as molecular and genetic characteristics among patients, which leads to distinct patterns of gene expression and signalling pathways. Understanding the SS heterogeneity at the omics level is vital in developing T-cell-mediated immunotherapeutic approaches, such as peptide-based vaccines.

HLA peptidomics refers to the study of the peptide repertoire presented by human leukocyte antigen (HLA) molecules [13–18]. These peptides are processed from intracellular proteins primarily by the proteasome and presented to the cell surface by HLA for T-cell recognition. HLA peptidomics enables the understanding of the mechanism of antigen processing and presentation in cancer cells. Including identification and characterisation of peptides from tumour-associated antigens (TAAs) and neoepitopes presented by HLA molecules on cancer cells. Overall, HLA peptidomics in cancer represents a powerful tool for understanding the mechanisms of antigen processing and presentation, highlighting potential tumour targets for T-cell-mediated immunotherapies.

HLA peptidomics studies for SS are warranted to determine how this SS heterogeneity impacts antigen processing and presentation, and to identify potential targets for SS T-cell-mediated immunotherapeutic vaccines. In this study, immunoaffinity purification of HLA-I peptide complexes from samples of SS clinical leukophoresis patients was carried out and analysed by high-performance liquid chromatography coupled to tandem mass spectrometry (HPLC-MS/MS). These HLA peptidomes were studied and compared in reference to presentation, lengths, subcellular locations, molecular/biological functions, and the top 20 genes with somatic mutation in SS as per the COSMIC database and whose protein HLA-I peptides were presented by all the four patients or at least 3 of the four patients (Rom, IrK, FrA and Seo); NCOR1, TRRAP, JAK3, PLCG1, TP53 and STAT3 (SAAs) analysed according to their immunogenicity, gene expression profiles, and protein interaction partners.

Materials and methods

Sezary Syndrome patients

The clinical leukapheresis material from 4 SS patients was used, with approval from the Charité ethics committee (Approval Nos. EA1/222/14 and EA1/026/14, dated 10/09/2014 and 28/02/2014, respectively) and written informed consent from

the volunteer donors. HLA type was determined by Charité – Universitätsmedizin Berlin, HLA typing laboratory.

Isolation and purification of MHC I-presented peptides

MHC class I molecules were isolated as described in detail elsewhere [19]. Briefly, cells were lysed in 20 mM Tris-HCl buffer, pH 7.4, containing 0.3% CHAPS, 0.2% NP-40, 145 mM NaCl, 1 mM EDTA, and 1 mM Pefabloc. Lysates were ultracentrifuged for 1h at 100,000 x g. The supernates were passed through a column with a monoclonal antibody of irrelevant specificity, followed by a column with the HLA-I anti-human monoclonal antibody (W6/32), both coupled to activated CH Sepharose as per the manufacturer's protocol (Amersham Biosciences AB, Uppsala, Sweden). After adsorption of the proteins, the anti-human HLA-I column was washed with the following in descending order: 20 mM Tris, 145 mM NaCl, pH 7.4 (TBS), 0.3% CHAPS in TBS, TBS, 0.3% ß-octylglycoside in TBS, TBS, and lastly with ultrapure H_2O. HLA-peptide complexes were eluted from the column with 0.7 % TFA in ultrapure H_2O. High-molecular-weight components were separated from peptides by centrifugal ultrafiltration using a molecular weight cutoff of 3 kDa (Centricon, Millipore, Schwalbach, Germany). The filtrates were fractionated on a Smart HPLC system (Amersham Biosciences, Freiburg, Germany) using a reverse phase column µRPC C2/C18, SC2.1/10 (Amersham Biosciences) and an acetonitrile gradient of 5–90% of B (solvent B: 0.1% TFA, 90% of acetonitrile; solvent A: 0.1% TFA in ultrapure H_2O). The fractions obtained were lyophilised and then re-dissolved in 0.1% TFA and 2% acetonitrile for LC-MS/MS analysis.

LC-MSMS analysis of HLA ligands

The peptide fractions were analysed by reversed-phase LC (Ultimate 3000 RSLCnano) coupled online with Q Exactive Plus MS (both, Thermo Fisher Scientific). Fractionated peptides were trapped on a C18 precolumn at 20 µL/min (2% acetonitrile, 0.1% TFA) for 4 min. Subsequently, peptides were separated at a flow rate of 300nl/min onto a 75-µm × 25 cm PepMap nano-HPLC column with a gradient of 3–30% of 80% acetonitrile and 0.1% FA acid in ultrapure H_2O over 90 min. Eluted peptides were nanospray-ionised and fragmented based on the ten most intense precursor ion signals, with a 20 sec dynamic exclusion time to avoid repeated fragmentation.

Data processing and analysis

The MS and MS/MS spectra were processed via Data Analysis (vers. 3.4) and Bio-tools (vers. 3.1) software (Bruker Daltonics). The local MASCOT server (vers. 2.2), utilising the Swissprot databank (vers. 56.3) for human proteins (20,408 reviewed entries), was used to identify the peptides. The precursor mass tolerance was 5 ppm for MS and 10 ppm for MS/MS, with methionine oxidation as a possible variable modification. For each peptide-spectrum match, candidate sequences were validated using a statistical evaluation -10logP, where logP is the logarithm to the base 10 of P ($P < 0.05$) as the absolute probability. Further validation of the identified peptides by *de novo* sequencing was performed using the Sequit software [20] and by manual inspection of the peptide-spectrum matches. The protein sequence, protein ID, and gene symbol for proteomic data analyses were extracted from the UniProt database [21]. The Human Protein Database [22] was used to classify proteins according to their subcellular location and biological function.

Somatic mutations.

To identify the top 20 genes with somatic mutations in SS, the Catalogue of Somatic Mutations in Cancer (COSMIC) was utilised https://cancer.sanger.ac.uk/cosmic [23]. The main search was set to SS, using the following browser filters: Tissue selection (Hematopoietic and lymphoid), Sub-tissue selection (All), Histology selection (lymphoid neoplasm) and Sub-histology selection (mycosis fungoides-sezary syndrome). In addition, the type of somatic mutation of the SAAs (The top 20 genes with somatic mutation in SS as per the COSMIC database and those whose HLA-I peptides were presented by all four patients or at least 3 of the four patients (Rom, IrK, FrA and Seo)) was also determined by COSMIC.

Sezary syndrome-associated antigens (SAAs) and their immunogenicity

To determine the immunogenicity of the SAAs, NetMHCpan 4.1 was used in the IEDB (http://www.iedb.org) [24]. The immunogenicity was determined for HLA-A*01:01, HLA-A*02:01,

HLA-A*11:01, HLA-A*24:02, HLA-C*06:02, HLA-C*07:01 and HLA-C*07:02, individually and all combined. These alleles are expressed together in 90% of the population [25]. IC50(500) nM binding affinity threshold was used as a threshold for immunogenicity, and immunogenicity scores were presented as 1/IC50(500) nM.

SAAs gene expression in primary normal human tissues, and protein interaction partners

To determine the gene expression profiles of the SAAs in normal major human tissues, the GeneCards database [26] was used, with a low gene expression intensity cut-off of 10%. The SAAs' protein interaction partners were determined using STRING version 11.5, a database of known and predicted protein-protein interactions [27]. STRING was used to determine known SAAs protein interaction partners, experimentally determined from various biochemical, biophysical and genetic techniques. A medium interaction score of 0.400 was applied, with a cut-off of 10 interaction partners at the primary level, against *Homo sapiens*.

Results

Naturally presented HLA I ligands of Sezary syndrome patients

The SS leukophoresis patient samples (Rom, IrK, FrA, and Seo) were lysed, and MHC class I molecules were isolated by affinity chromatography. LC-MS/MS then analysed peptides extracted from the MHC molecules. The sequences of a total of 7668, 8492, 8123, and 4854 HLA class I-bound peptides were identified from 3003, 4027, 3865, and 2390 source proteins in Rom, IrK, FrA, and Seo, respectively (see **Figure 1A**). 6086, 7512, 6905, and 3441 HLA class I-bound peptides were unique in Rom, IrK, FrA, and Seo, respectively (see **Figure 1A**). The shared peptides between patients ranged from 146 (0.6%) to 748 (2.8%), and were

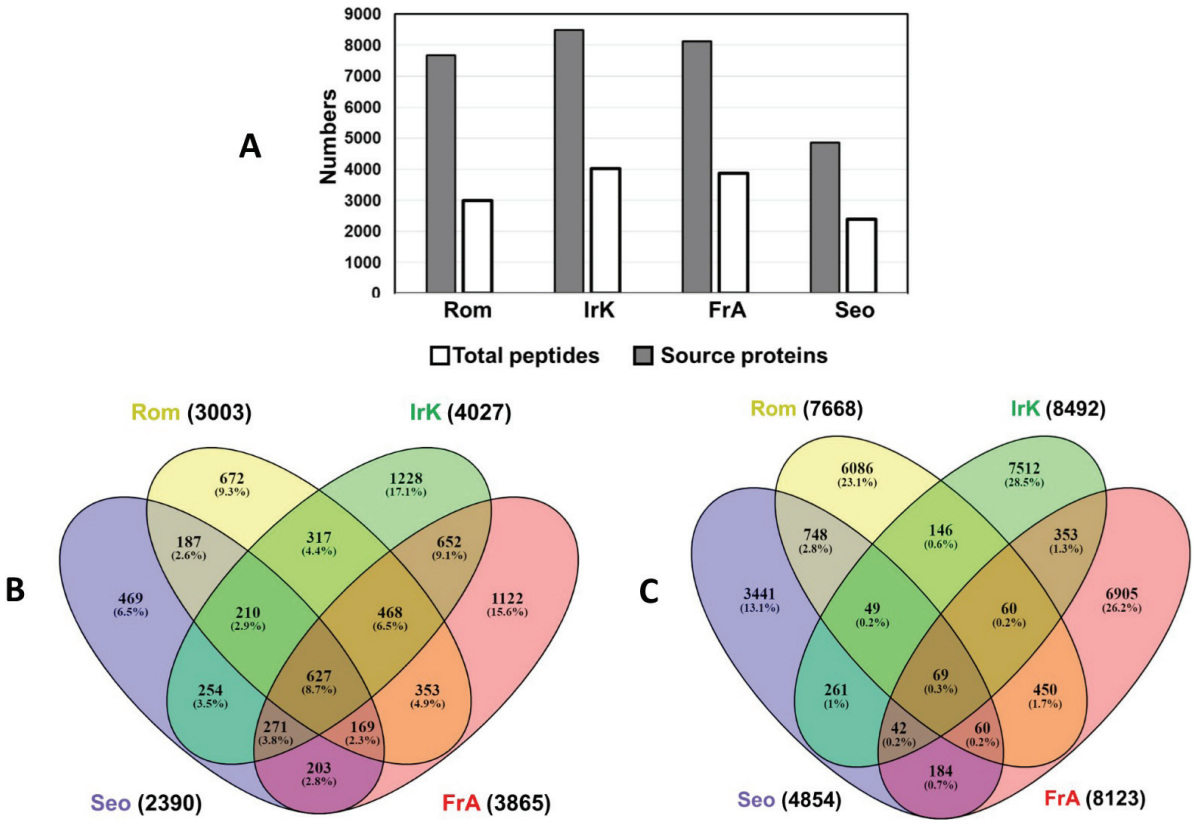

Figure 1. Naturally presented HLA class I ligands and Source proteins of Sezary syndrome leukapharesis patients' samples. The leukapharesis samples were lysed, MHC I molecules were isolated by affinity chromatography, and LC-MS/MS analysed peptides extracted from the MHC molecules. A) Number of naturally presented HLA class I ligands and Source proteins. B) Shared-Naturally presented HLA class I ligands. C) Shared- Naturally presented HLA class I ligand source proteins.

well below 1% among the patients. Only 69 (0.3%) HLA I peptide sequences were found to be shared among all four patients based only on peptide sequences. Precursor peptide mass signals and retention time, respectively (see **Figure 1B**). The HLA expression was HLA-A2, HLA-A24, HLA-B7 and HLA-B8, HLA-C6 and HLA-C7 in Seo, HLA-A1, HLA-A33, HLA-B8, HLA-B14, HLA-C7 and HLA-C8 in Rom, while the HLA expression in IrK and FrA was undetermined. The shared proteins between the patients ranged from 187 (2.6%) to 652 (9.1%), with only 627 (8.7%) shared among the four patients (see **Figure 1C**).

MHC I-bound peptide lengths and C-Terminus processing

The MHC I-bound peptide lengths in all patients were dominated by nanopeptides, constituting 29.0% to 55.1% of all identified peptides. At the same time, decapeptides were the second dominant, constituting 8.0% – 14.8%. Undecapeptides and above, on the other hand, were less than 11% in all patients (see **Figure 2**). The C-terminus peptide processing by the proteasome, based on peptide numbers and percentages, was Chymotrypsin > Trypsin > Caspase in all patients (see **Figure 3).**

Sub-cellular locations and molecular functions of source proteins

The human protein reference database was used to assign the subcellular location of the source proteins of the HLA I-bound peptides from Rom, IrK, FrA and Seo. The cytoplasm, intracellular membrane-bounded organelles, and cytosol were the dominant subcellular locations of the source

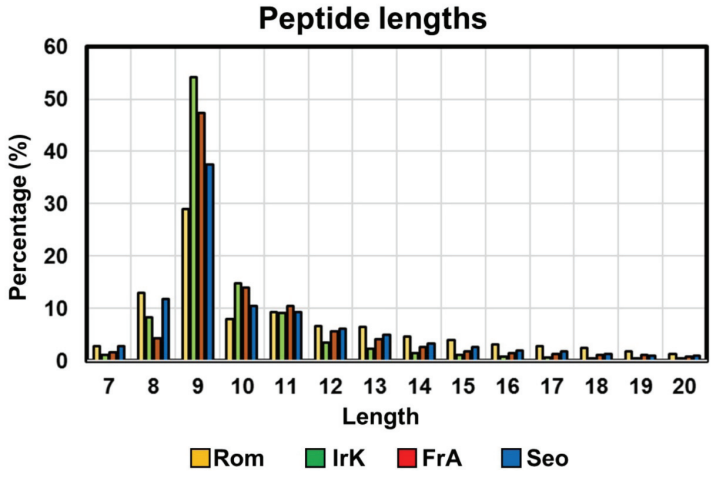

Figure 2. MHC Class I -peptide lengths in Sezary syndrome Leukapheresis patients' samples.

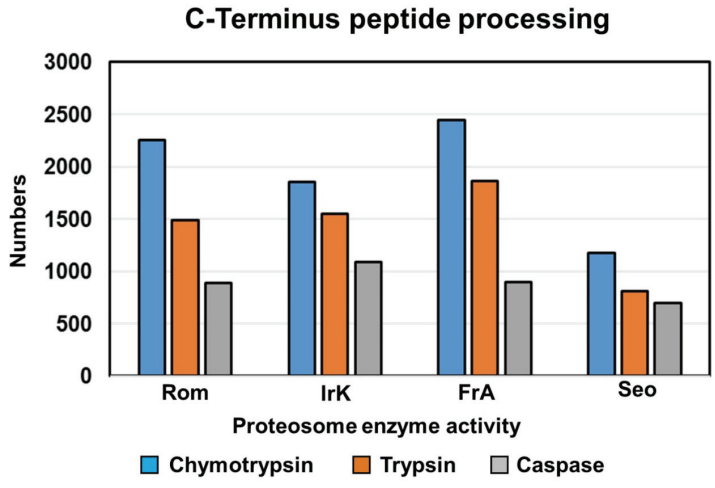

Figure 3. MHC Class I –peptides C-Terminus processing by the proteasome.

proteins (see **Figure 4**). Together, they accounted for 29.6%, 28.8%, 27.1%, and 24.7% of all the source proteins in Rom, IrK, FrA, and Seo, respectively. Approximately half of this percentage was solely from the cytoplasmic part, which accounted for more than 14% of all the source proteins. Source proteins from the cell junction were 10.3% in Seo, considerably higher compared to those in Rom, Irk, and FrA, which were 3.9%, 3.9%, and 3.3%, respectively. Source proteins' subcellular locations were lowest in the condensed chromosome, endoplasmic reticulum lumen, and intracellular organelle lumen in all patients, with values ranging from 0% to 0.32% (data not shown). The source proteins originated from diverse subcellular locations in all patients (see **Figure 4**). These proteins were further evaluated for their biological/molecular functions, using the human protein reference database [22]. Although source proteins possessed multiple biological/molecular functions, a vast majority were involved in biosynthetic process (14.7%, 13.4%, 12.0%, 11.6%), biological regulation (8.9%, 10.0%, 10.5%, 11.1%), catabolic process (8.1%, 5.3%, 4.8%, 5.6%) and anatomical structure development (5.3%, 4.1%, 4.6%, 4.4%) in Rom, IrK, FrA and Seo respectively (see **Figure 5**). They were also those involved in immune response, cell death and apoptosis, but were below 2% in all patients.

Somatic mutations in cosmic

To determine the top 20 genes with somatic mutations in SS, the Catalogue of Somatic Mutations in Cancer (COSMIC) was used. The top 20 genes with somatic mutation as per COSMIC, search filtered as follows; tissue (hematopoietic and lymphoid), sub-tissue (All), histology (lymphoid neoplasm) and sub-histology (mycosis fungoides-sezary syndrome) were Fat Atypical Cadherin 4 (*FAT4*), Fat Atypical Cadherin 1 *(FAT1*), Caspase Recruitment Domain Family Member 11 (*CARD11*), Nuclear Receptor Corepressor 1 (*NCOR1*), Phospholipase C Gamma 1 (*PLCG1*), Tumor Protein P53 (*TP53*), Glutamate Ionotropic Receptor NMDA Type Subunit 2A (*GRIN2A*), AT-Rich Interaction Domain 1A (*ARID1A*), LDL Receptor Related Protein 1B (*LRP1B*), phosphatidylinositol-3,4,5-trisphosphate dependent rac exchange factor 2 (*PREX2*),

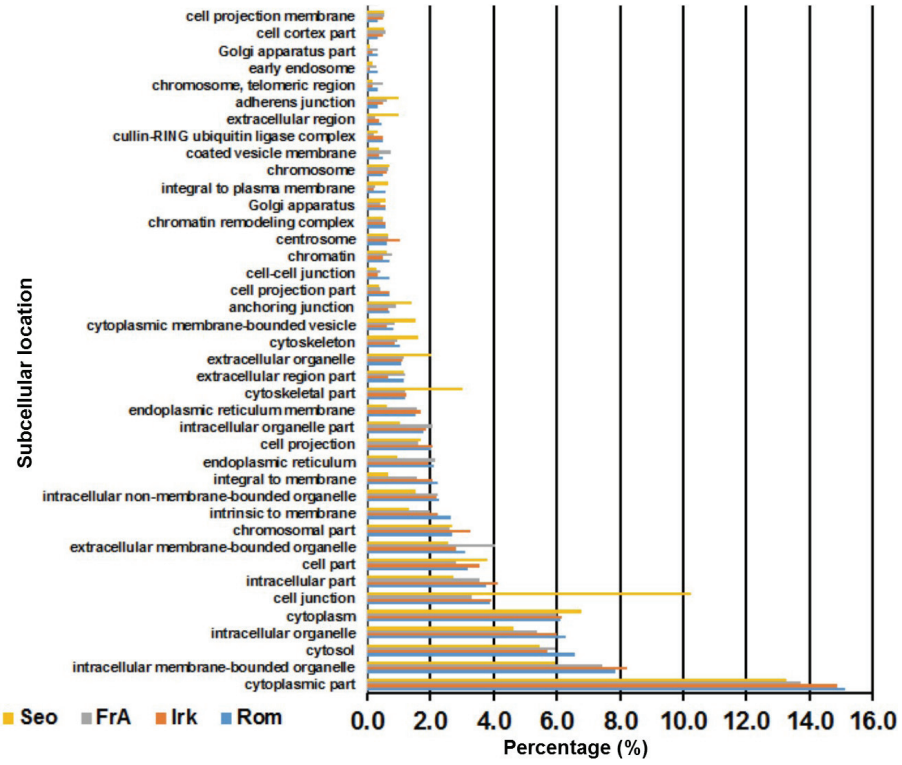

Figure 4. Subcellular location of the source proteins. The subcellular locations of the source proteins of the HLA class I-bound peptides from Sezary syndrome leukapheresis patients' samples identified by mass spectrometry were assigned using the Human Protein Reference Database.

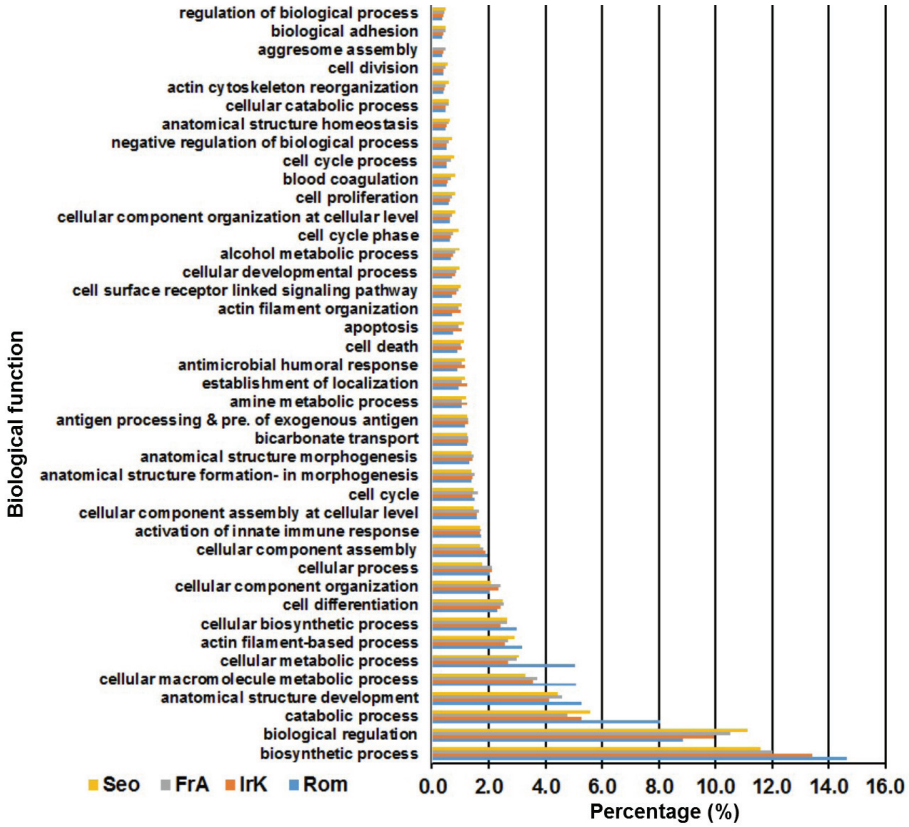

Figure 5. Biological/molecular functions of the source proteins. The biological/molecular functions of the source proteins of the HLA class I-bound peptides from Sezary syndrome Leukapheresis patients' samples were assigned using the Human Protein Reference Database.

Protection of Telomeres 1 (*POT1*), Tet Methylcytosine Dioxygenase 2 (*TET2*), DNA Methyltransferase 3 Alpha (*DNMT3A*), Protein Tyrosine Phosphatase Receptor Type K (*PTPRK*), Erb-B2 Receptor Tyrosine Kinase 4 (*ERBB4*), Signal Transducer and Activator of Transcription 5B (*STAT5B*), Transformation/Transcription Domain Associated Protein (*TRRAP*), Janus Kinase 3 (*JAK3*), Platelet-Derived Growth Factor Receptor Alpha (*PDGFRA*) and Signal Transducer and Activator of Transcription 3 (*STAT3*) with mutation frequencies of 16%, 15%, 14%, 14%, 14%, 13%, 11%, 10%, 10%, 10%, 8%, 8%,7%,7%, 6%, 5%, 5%, 4%, 4%, and 4% respectively, from the all the tumors samples (see **Figure 6A**). HLA-I peptides from NCOR1, TRRAP and JAK3 were presented by all the four patients Rom, IrK, FrA and Seo. PLCG1, TP53, and STAT3 were altered in at least three of the four patients, while FAT1 and LRP1B were changed in at least two of the four patients, and FAT4, TET2, and PTPRK were altered in at least one of the four patients. No HLA-I peptides was presented from FAT4, CARD11, GRIN2A, ARID1A, PREX2, POT1, DNMT3A, ERBB4, STAT5B and PDGFRA (see **Figure 6B**). The somatic in the SAAs (the top 20 genes with somatic mutation in SS as per the COSMIC database and those whose HLA-I peptides were presented by all the four patients or at least 3 of the four patients (Rom, IrK, FrA and Seo), that include *NCOR1, TRRAP, JAK3, PLCG1, TP53* and *STAT3*), were predominantly missense variant (a type of substitution in which the nucleotide change results in the replacement of one amino acid with another, a replacement that may alter the function of the protein). With mutation frequencies of 46.7%, 60.0%, 100%, 94.74%, 52.4% and 70% respectively. Nonsense mutations (that occur due to the substitution of a single base pair in a triplet codon), leading to one of three stop codons (UAG, UAA, and UGA). The triplet codon coding for an amino acid is therefore altered to one that prematurely stops mRNA translation and results in a truncated protein. They were found only in *NCOR1* and *TP53*, with frequencies of 20% and 23%, respectively (data not shown).

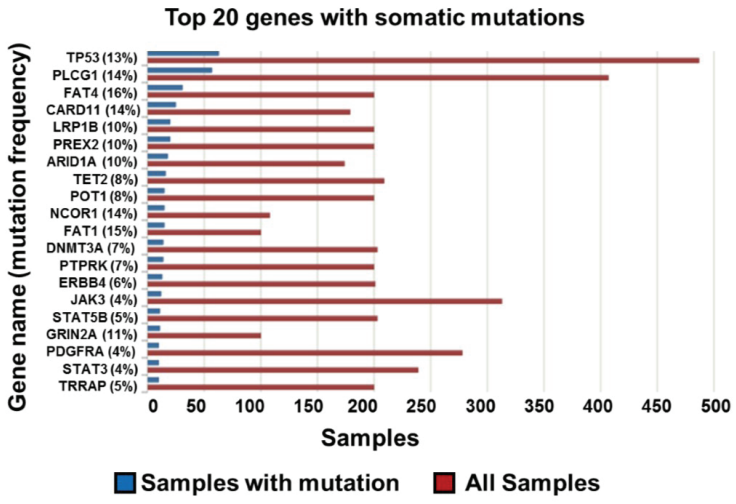

Gene	Mutation frequency	Patient			
		Rom	IrK	Seo	FrA
NCOR1	14%	x	x	x	x
TRRAP	5%	x	x	x	x
JAK3	4%	x	x	x	x
PLCG1	14%	x	x		x
TP53	13%	x	x	x	
STAT3	4%	x		x	x
FAT1	15%	x			x
LRP1B	10%		x		x
FAT4	16%		x		
TET2	8%		x		
PTPRK	7%	x			
CARD11	14%				
GRIN2A	11%				
ARID1A	10%				
PREX2	10%				
POT1	8%				
DNMT3A	7%				
ERBB4	6%				
STAT5B	5%				
PDGFRA	4%				

A B

Figure 6. Top 20 genes with somatic mutation in Sezary syndrome as per catalogue of Somatic mutations in Cancer (COSMIC). A) COSMIC search set to Sezary syndrome, and filtered by tissue selection (hematopoietic and lymphoid), Sub-tissue selection (All), Histology selection (lymphoid neoplasm) and Sub-histology selection (mycosis fungoides-sezary syndrome). B) Frequency of somatic mutation of the SAAs (the top 20 genes with somatic mutation in Sezary syndrome as per the COSMIC database and HLA-I peptides presentation from the SAAs by the patients (Rom, IrK, FrA and Seo).

Immunogenicity of the LAAs

The immunogenicity of the SAAs (the top 20 genes with somatic mutation in SS as per the COSMIC database and whose protein HLA-I peptides were presented by all four patients or at least 3 of the four patients (Rom, IrK, FrA and Seo); NCOR1, TRRAP, JAK3, PLCG1, TP53 and STAT3) was determined by reverse immunology. NetMHCpan 4.1 BA in the IEDB was used with a binding affinity threshold of IC_{50} (500 nM), for the most frequent HLA alleles HLA-A*01:01, HLA-A*02:01, HLA-A*11:01, HLA-A*24:02, HLA-C*06:02, HLA-C*07:01 and HLA-C*07:02 that together represent ~90% of the human population. The immunogenicity score is represented as $1/IC_{50}$ (500 nM) and ranges from 0 to 1, indicating low to high immunogenicity. The immunogenicity of the SAAs varied depending the HLA allele (see **Figure 7**). It was generally highest for HLA-A*11:01 and HLA-A*02:01 and lowest for HLA-A*01:01. The immunogenicity of SAAs for all the alleles was comparable, with median score of less than 0.2 for HLA-A*11:01 and HLA-A*02:01 alleles, and less than 0.4 for all the other alleles, except HLA-A*01:01 which ranged between 0.1 and 0.6. TRRAP had the highest number of peptides within this binding affinity threshold of IC50 (500 nM).

SAA gene expression in major normal tissues

The gene expression profiles of the SAAs in primary normal human tissues were compared using the GeneCards database, as detailed in the Materials and Methods section. All the SAAs were expressed at low levels in all primary normal human tissues based on a 10% gene expression intensity cutoff. Only *STAT3* were expressed beyond the 10% cutoff. Beyond this cutoff, *STAT3* was expressed in whole blood, thymus, adipocyte, lung and prostate (see **Figure 8**).

Protein interaction partners of the LAAs

High numbers of protein interaction partners and the interaction of SAAs (NCOR1, TRRAP, JAK3, PLCG1, TP53 and STAT3) between and among them may indicate vital roles in SS. The STRING database was used to determine the protein interaction partners of the SAAs, which had been initially identified from experimental data obtained using a variety of biochemical, biophysical, and genetic techniques, as detailed in the Materials and Methods section. All SAAs (NCOR1, TRRAP, JAK3, PLCG1, TP53 and STAT3) had ten known interaction partners (see **Figure 9**). None of the SAAs were found to interact with each other, both

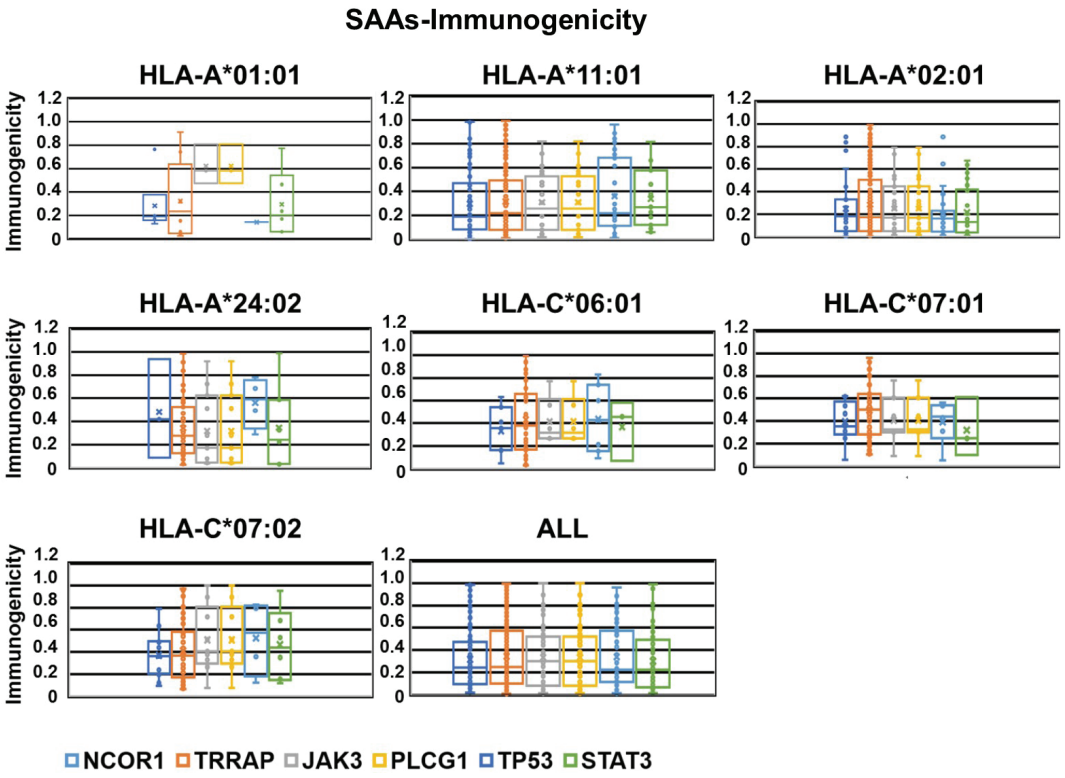

Figure 7. Immunogenicity of the SAAs for the most frequent HLA alleles, HLA-A*01:01, HLA-A*02:01, HLA-A*11:01, HLA-A*24:02, HLA-C*06:02, HLA-C*07:01, and HLA-C*07:02, which together represent more than 90% of the human population. The immunogenicity was determined using NetMHCpan 4.0 in IEDB [64], with a binding affinity threshold of IC_{50} (500 nM). The immunogenicity scores are presented as $1/IC_{50}$ (500 nM), with values ranging from 0 to 1, indicating low to high immunogenicity.

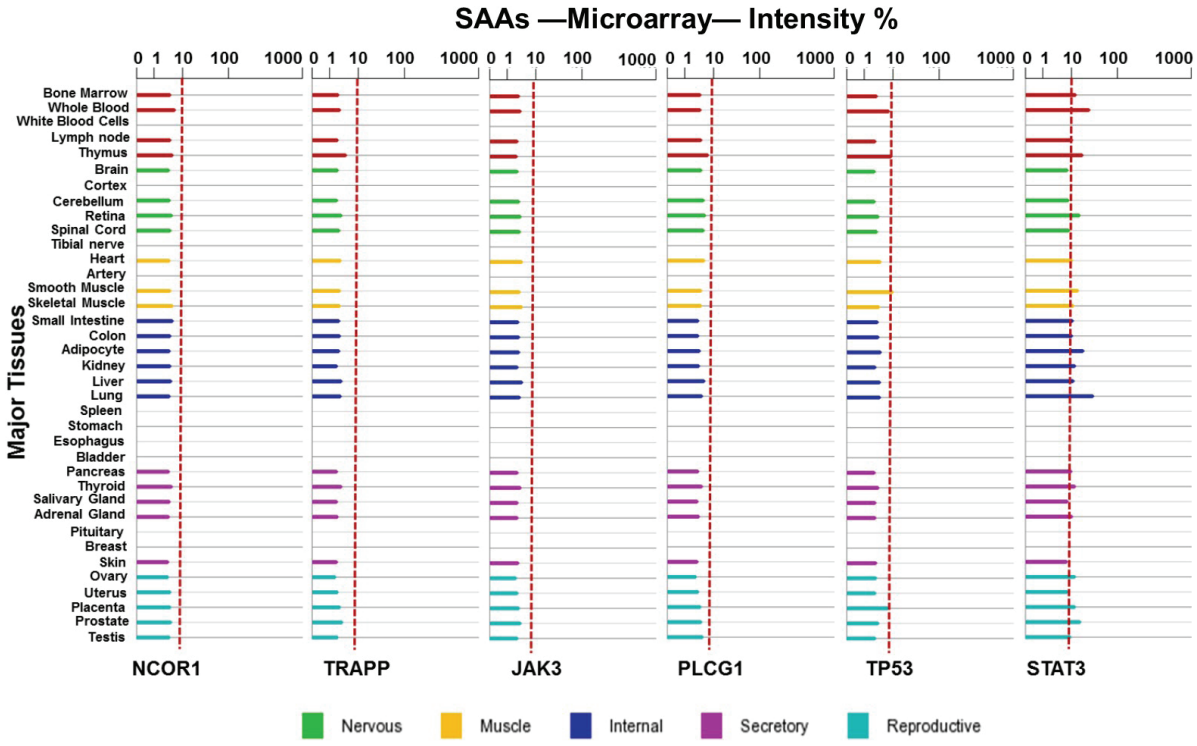

Figure 8. Gene expression profiles of the SAAs in normal human tissue were analysed and visualised using BioGPS (http://biogps.org). A low gene expression intensity cutoff of 10% indicated by the dotted line.

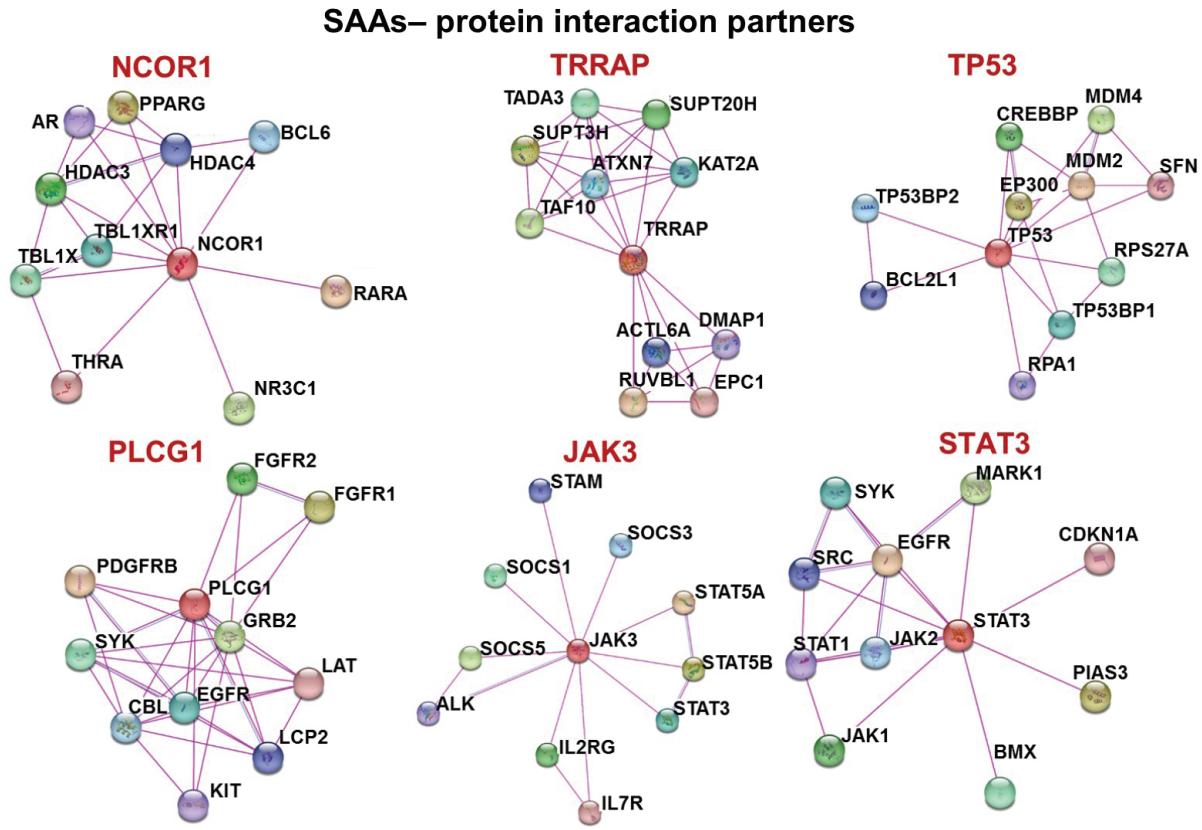

Figure 9. Known protein interaction partners of the SAAs were determined using STRING version 11.0 [66] for *Homo sapiens* with a medium score of 0.400 and a cutoff of 10 interaction partners.

at primary (directly via the first shell) (see **Figure 9**) and at secondary level (indirectly via the second shell) (data not shown), except JAK3 and STAT3, which interacted at the primary level.

Discussion

The total number of HLA-I–restricted peptides and source proteins identified in SS leukophoresis patient samples was about the same, and they were heterogeneous and individualised (see **Figure 1A**, **B** and **C**). Only a small fraction of HLA-I peptides and source proteins was found to be shared between and among the patients (see **Figure 1B** and **C**). The HLA-I–bound peptides were more heterogeneous and individualised than the source proteins, as the number of shared HLA-I peptides was slightly lower compared with that of the source proteins. This has also been observed in other human cell lines and tumour samples, such as melanoma, and depicts differences in the antigen processing and presentation in SS. In this case, the HLA-I peptides may also be attributed to the difference in the patient's HLA type, although this has not been fully confirmed.

Despite the fact that the HLA-I peptides and the source proteins were heterogeneous and individualised, a number of similarities were observed. First, in all SS leukophoresis patients' samples, nanopeptides were the most dominant and constituted between 29.0% to 55.1% of all the peptides identified, followed by decapeptides with 8.0% to 14.8% (see **Figure 2**). This dominance of nanopeptides has also been observed in other patient tumour samples and cell lines [19,28–31]. It indicates that the optimum length for MHC I-binding peptides in SS is nine amino acids. Secondly, the proteasome activity, in reference to C-terminus peptide processing, was found to be decreasing in activity with chymotrypsin, trypsin, and, lastly, caspase in all patients (see **Figure 3**).

Similarities were also observed in the HLA-I peptides of SS patients, their source proteins, subcellular locations, and molecular functions. The cytoplasm part, intracellular membrane-bounded organelle and cytosol were the

dominant subcellular locations of the source proteins (see **Figure 4**). Together, they accounted for 24.7% to 29.6 %, with the cytoplasmic part accounting for more than 14% of all the source proteins. This is different to the dominant subcellular locations of the HLA-I peptide source proteins of other human tumor samples and cell lines such as melanoma, multiple sclerosis autopsy samples, B lymphoblastic cell line, tipple- negative breast cancer cell line, leukemia tumuor samples and cell lines; where the dominant subcellular locations differed and varied e.g. in melanoma the dominant subcellular locations were the nucleus and the cytoplasm, multiple sclerosis autopsy samples, where cytoplasm and plasma membrane [19,28–32].

Second, the source proteins were involved in various molecular functions, especially in biosynthetic processes, biological regulation, catabolic processes, and anatomical structure development, with a similar proportion of proteins per molecular function (see **Figure 5**). This is different from other human tumour samples and cell lines. For instance, in leukaemia cell lines MUTZ3 and THP1, the source proteins were involved in cell communication/signal transduction, protein metabolism, and transcription factor activity/regulator activity [19]. In the B lymphoblastic cell line 721.221, the source proteins were predominantly involved in metabolism, cell growth and maintenance, cell communication, and stress response [30]. In multiple sclerosis autopsy samples, they entailed cellular assembly and organisation, nervous system function and development, cellular growth, and proliferation [31]. The similarities in source protein peptide sampling in SS, although unconfirmed, would imply similarities in protein turnover, because protein turnover correlates with source protein peptide sampling [33,34]. The availability of source proteins involved in immune response, apoptosis, and cell death in all patients would indicate an active immune response against the cancer cells by the patients.

Furthermore, the top 20 genes with somatic mutation in SS were *FAT4, FAT1, CARD11, NCOR1, PLCG1, TP53, GRIN2A, ARID1A, LRP1B, PREX2, POT1, TET2, DNMT3A, PTPRK, ERBB4, STAT5B, TRRAP, JAK3, PDGFRA* and *STAT3*, as per COSMIC, with decreasing mutation frequencies of 16% to 4% (see **Figure 6A**). Out of these, only HLA-I peptides from NCOR1, TRRAP and JAK3 were presented by all the four patients, PLCG1, TP53 and STAT33 by three of the four patients, FAT1 and LRP1B by two of the four patients, TET2 and PTPRK by one of the four patients. No HLA-I peptides were presented from FAT4, CARD11, GRIN2A, ARID1A, PREX2, POT1, DNMT3A, ERBB4, STAT5B and PDGFRA (see **Figure 6B**). The missense mutation was the predominant mutation, with mutation frequency ranging between 46.7% to 100% in the top 20 genes sampled by at least three of the four patients (see **Supplementary Figure 1**). Nonsense mutations were found only in *NCOR1* and *TP53*, with mutation frequency of 20% and 23% respectively (see **Supplementary Figure 1**). These mutation finding highlights the genetic heterogeneity of SS and points to *NCOR1, TRRAP, JAK3, PLCG1, TP53* and *STAT3* (the SAAs) as initial potential targets for T-cell based immunotherapeutic intervention, based on their high mutation rate and their protein HLA-I peptide presentation by at least three of the four patients. This is further substantiated by previous studies showing that SAAs are key regulators in various stages of cancer progression and are critical therapeutic targets. NCOR1 promotes cancer progression and therapy resistance by dysregulating transcriptional networks [35–41]. TRAPP promotes cancer development and progression by enhancing cancer stem cell traits, suppressing immune responses, regulating oncogenic transcription factors, and supporting cancer cell proliferationsupport [42–46]. JAK3 promotes the proliferation and survival of malignant T-cells and influences immune suppression [47–52]. PLCG1 promotes progression by supporting tumour growth and therapy resistance (53,54). TP53 mutations impair tumour suppression and contribute to therapy resistance and poor prognosis [53–59]. STAT3 promotes tumour cell survival, proliferation, immune evasion, and therapy resistance (62–64).

Furthermore, the immunogenicity of these SAAs (NCOR1, TRRAP, JAK3, PLCG1, TP53 and STAT3) was allele-dependent. It was generally highest for HLA-A*11:01 and HLA-A*02:01 and lowest for HLA-A*01:01 (see **Figure 7**). The immunogenicity of SAAs for all the alleles was comparable, with TRRAP showing the highest number of affinity peptides. These findings suggest that specific alleles may play a crucial role in shaping the immune response to SAAs in SS, with

implications for personalised immunotherapy approaches. Regarding the gene expression profile of the SAAs in normal human tissues, expression levels were generally low, except for STAT3 in certain tissues (see **Figure 8**). Therefore, targeting *STAT3* in SS immunotherapy may lead to off-target effects in these select tissues. Regarding the protein interaction partners, all SAAs exhibited a high number of protein interaction partners, emphasising their vital roles in SS (see **Figure 9**). With only JAK3 and STAT3 interacting with each other at the primary level, this interaction warrants further investigation to determine its role in SS.

Overall, despite the small patient sample size and limited demographics, this study's findings primarily contribute to our understanding of the peptidomic landscape in SS and highlight SAAs (NCOR1, TRRAP, JAK3, PLCG1, TP53) as potential targets for immunotherapeutic interventions. The immunotherapeutic potential is based on the SAAs high mutation rate in SS, HLA-I peptides presentation, high immunogenicity, low gene expression profiles in normal human tissue, and a high number of protein interaction partners. Including their role in cancer, as mentioned in the previous studies above. *STAT3* falls short in the SAAs list, as it is also highly expressed in some normal human tissues. However, its interaction with JAK3 at the primary level warrants future studies to determine the role of this interaction.

Disclosures

Author contributions
L.W.N. conceived the project, designed and performed the experiments, analysed and interpreted results, and wrote the paper. K.T-T contributed to the generation of LC-MS/MS data. P.W. conceived the project, contributed reagents/materials, and contributed to the interpretation of the results. All authors reviewed the results and approved the manuscript.

Conflict of interest statement
The authors declare no conflict of interest.

Funding sources
The study was supported by funds from the German Ministry for Research and Education (BMBF, 13N9197), the Berlin Cancer Society (WAFF200824), and the German Academic Exchange Service (DAAD). Many thanks to Dr. med. Christoph Gille, at the Institute of Biochemistry, Charité-Universitätsmedizin Berlin, for his support in Analysing Sub-Cellular locations and molecular functions of source proteins.

References

1. Alaggio R, Amador C. The 5th edition of the World Health Organization Classification of Haematolymphoid Tumours: Lymphoid Neoplasms. Leukemia. 2022;36:1720–48. https://doi.org/10.1038/s41375-022-01620-2.
2. Willemze R, Cerroni L, Kempf W, Berti E, Facchetti F. The 2018 update of the WHO-EORTC classification for primary cutaneous lymphomas. Blood. 2019;133:1703–14. https://doi.org/10.1182/blood-2018-11-881268.
3. Agar NS, Wedgeworth E, Crichton S, Mitchell TJ, Cox M, Ferreira S, et al. Survival outcomes and prognostic factors in mycosis fungoides/Sézary syndrome: validation of the revised International Society for Cutaneous Lymphomas/European Organisation for Research and Treatment of Cancer staging proposal. J Clin Oncol. 2010;28:4730–9. https://doi.org/10.1200/jco.2009.27.7665.
4. Scarisbrick JJ, Prince HM, Vermeer MH, Quaglino P, Horwitz S, Porcu P, et al. Cutaneous Lymphoma International Consortium Study of Outcome in Advanced Stages of Mycosis Fungoides and Sézary Syndrome: Effect of Specific Prognostic Markers on Survival and Development of a Prognostic Model. J Clin Oncol. 2015;33:3766–73. https://doi.org/10.1200/jco.2015.61.7142.
5. Jawed SI, Myskowski PL, Horwitz S, Moskowitz A, Querfeld C. Primary cutaneous T-cell lymphoma (mycosis fungoides and Sézary syndrome): part II. Prognosis, management, and future directions. J Am Acad Dermatol. 2014;70:223.e1-17; quiz 240–2. https://doi.org/10.1016/j.jaad.2013.08.033.
6. Querfeld C, Zain J, Rosen ST. Primary Cutaneous T-Cell Lymphomas: Mycosis Fungoides and Sezary Syndrome. Cancer Treat Res. 2019;176:225–48. https://doi.org/10.1007/978-3-319-99716-2_11.
7. Stuver R, Geller S. Advances in the treatment of mycoses fungoides and Sézary syndrome: a narrative update in skin-directed therapies and immune-based treatments. Front Immunol. 2023;14:1284045. https://doi.org/10.3389/fimmu.2023.1284045.
8. Roccuzzo G, Giordano S, Fava P, Pileri A, Guglielmo A, Tonella L, et al. Immune Check Point Inhibitors in Primary Cutaneous T-Cell Lymphomas: Biologic Rationale, Clinical Results and Future Perspectives. Front Oncol. 2021;11:733770. https://doi.org/10.3389/fonc.2021.733770.
9. Larocca C, Kupper T. Mycosis Fungoides and Sézary Syndrome: An Update. Hematol Oncol Clin North Am. 2019;33:103–20. https://doi.org/10.1016/j.hoc.2018.09.001.
10. Buus TB, Willerslev-Olsen A. Single-cell heterogeneity in Sézary syndrome. Blood Advances. 2018;2:2115–26. https://doi.org/10.1182/bloodadvances.2018022608.
11. Litvinov IV, Tetzlaff MT, Thibault P, Gangar P, Moreau L, Watters AK, et al. Gene expression analysis in Cutaneous T-Cell Lymphomas (CTCL) highlights disease heterogeneity and potential diagnostic and prognostic indicators. Oncoimmunology. 2017;6:e1306618. https://doi.org/10.1080/2162402x.2017.1306618.

12. Vergnolle I, Douat-Beyries C, Boulinguez S, Rieu JB. CD158k and PD-1 expressions define heterogeneous subtypes of Sezary syndrome. Blood Advances. 2022;6:1813–25. https://doi.org/10.1182/bloodadvances.2021005147.
13. Bassani-Sternberg M, Bräunlein E, Klar R, Engleitner T, Sinitcyn P, Audehm S, et al. Direct identification of clinically relevant neoepitopes presented on native human melanoma tissue by mass spectrometry. Nat Commun. 2016;7:13404. https://doi.org/10.1038/ncomms13404.
14. Caron E, Kowalewski DJ, Chiek Koh C, Sturm T, Schuster H, Aebersold R. Analysis of Major Histocompatibility Complex (MHC) Immunopeptidomes Using Mass Spectrometry. Mol Cell Proteomics. 2015;14:3105–17. https://doi.org/10.1074/mcp.O115.052431.
15. Hellinger R, Sigurdsson A. Peptidomics. Nature Reviews Methods Primers. 2023;3.25 https://doi.org/10.1038/s43586-023-00205-2.
16. Kalaora S, Barnea E, Merhavi-Shoham E, Qutob N, Teer JK, Shimony N, et al. Use of HLA peptidomics and whole exome sequencing to identify human immunogenic neo-antigens. Oncotarget. 2016;7:5110–7. https://doi.org/10.18632/oncotarget.6960.
17. Shapiro IE, Bassani-Sternberg M. The impact of immunopeptidomics: From basic research to clinical implementation. Semin Immunol. 2023;66:101727. https://doi.org/10.1016/j.smim.2023.101727.
18. Vaughan K, Xu X, Caron E, Peters B, Sette A. Deciphering the MHC-associated peptidome: a review of naturally processed ligand data. Expert Rev Proteomics. 2017;14:729–36. https://doi.org/10.1080/14789450.2017.1361825.
19. Nyambura LW, Jarmalavicius S, Baleeiro RB. Diverse HLA-I Peptide Repertoires of the APC Lines MUTZ3-Derived Immature and Mature Dendritic Cells and THP1-Derived Macrophages. The Journal of Immunology. 2016;197:2102–9. https://doi.org/10.4049/jimmunol.1600762.
20. Demine R, Walden P. Sequit: software for de novo peptide sequencing by matrix-assisted laser desorption/ionization post-source decay mass spectrometry. Rapid Commun Mass Spectrom RCM. England; 2004;18:907–13. https://doi.org/10.1002/rcm.1420.
21. UniProt: the Universal Protein Knowledgebase in 2023. Nucleic Acids Res. England; 2023;51:D523–31. https://doi.org/10.1093/nar/gkac1052.
22. Mishra GR, Suresh M, Kumaran K, Kannabiran N, Suresh S, Bala P, et al. Human protein reference database--2006 update. Nucleic Acids Res. 2006;34:D411-4. https://doi.org/10.1093/nar/gkj141.
23. Sondka Z, Dhir NB, Carvalho-Silva D. COSMIC: a curated database of somatic variants and clinical data for cancer. Nucleic Acids Research. 2024;52:D1210-d1217. https://doi.org/10.1093/nar/gkad986.
24. Vita R, Mahajan S, Overton JA, Dhanda SK, Martini S, Cantrell JR, et al. The Immune Epitope Database (IEDB): 2018 update. Nucleic Acids Res. England; 2019;47:D339–43. https://doi.org/10.1093/nar/gky1006.
25. Gonzalez-Galarza FF, McCabe A, Santos E, Jones J, Takeshita L, Ortega-Rivera ND, et al. Allele frequency net database (AFND) 2020 update: gold-standard data classification, open access genotype data and new query tools. Nucleic Acids Res. 2020;48:D783-d788. https://doi.org/10.1093/nar/gkz1029.
26. Stelzer G, Rosen N, Plaschkes I, Zimmerman S, Twik M, Fishilevich S, et al. The GeneCards Suite: From Gene Data Mining to Disease Genome Sequence Analyses. Curr Protoc Bioinforma. United States; 2016;54:1.30.1-1.30.33. https://doi.org/10.1002/cpbi.5.
27. Szklarczyk D, Gable AL, Lyon D, Junge A, Wyder S, Huerta-Cepas J, et al. STRING v11: protein-protein association networks with increased coverage, supporting functional discovery in genome-wide experimental datasets. Nucleic Acids Res. England; 2019;47:D607–13. https://doi.org/10.1093/nar/gky1131.
28. Jarmalavicius S, Welte Y, Walden P. High immunogenicity of the human leukocyte antigen peptidomes of melanoma tumor cells. J Biol Chem. 2012;287:33401–11. https://doi.org/10.1074/jbc.M112.358903.
29. Pritchard AL, Hastie ML, Neller M, Gorman JJ, Schmidt CW, Hayward NK. Exploration of peptides bound to MHC class I molecules in melanoma. Pigment Cell Melanoma Res. 2015;28:281–94. https://doi.org/10.1111/pcmr.12357.
30. Schellens IM, Hoof I, Meiring HD, Spijkers SN, Poelen MC, van Gaans-van den Brink JA, et al. Comprehensive Analysis of the Naturally Processed Peptide Repertoire: Differences between HLA-A and B in the Immunopeptidome. PLoS One. 2015;10:e0136417. https://doi.org/10.1371/journal.pone.0136417.
31. Fissolo N, Haag S, de Graaf KL, Drews O, Stevanovic S, Rammensee HG, et al. Naturally presented peptides on major histocompatibility complex I and II molecules eluted from central nervous system of multiple sclerosis patients. Mol Cell Proteomics. 2009;8:2090–101. https://doi.org/10.1074/mcp.M900001-MCP200.
32. Brito Baleeiro R, Liu P, Chard Dunmall LS, Di Gioia C, Nagano A, Cutmore L. Personalized neoantigen viro-immunotherapy platform for triple-negative breast cancer. Journal for ImmunoTherapy of Cancer. 2023;11:e007336. https://doi.org/10.1136/jitc-2023-007336.
33. Bassani-Sternberg M, Pletscher-Frankild S, Jensen LJ, Mann M. Mass spectrometry of human leukocyte antigen class I peptidomes reveals strong effects of protein abundance and turnover on antigen presentation. Mol Cell Proteomics. 2015;14:658–73. https://doi.org/10.1074/mcp.M114.042812.
34. Rock KL, Farfán-Arribas DJ, Colbert JD, Goldberg AL. Re-examining class-I presentation and the DRiP hypothesis. Trends Immunol. 2014;35:144–52. https://doi.org/10.1016/j.it.2014.01.002.
35. Abedin SA, Thorne JL, Battaglia S, Maguire O, Hornung LB, Doherty AP, et al. Elevated NCOR1 disrupts a network of dietary-sensing nuclear receptors in

bladder cancer cells. Carcinogenesis. 2009;30:449–56. https://doi.org/10.1093/carcin/bgp005.
36. Fozzatti L, Park JW, Zhao L, Willingham MC, Cheng SY. Oncogenic Actions of the Nuclear Receptor Corepressor (NCOR1) in a Mouse Model of Thyroid Cancer. PLoS One. 2013;8:e67954. https://doi.org/10.1371/journal.pone.0067954.
37. Kim H, Park SH. TNFα Enhances Tamoxifen Sensitivity through Dissociation of ERα-p53-NCOR1 Complexes in ERα-Positive Breast Cancer. Cancers. 2021;13(11):2601. https://doi.org/10.3390/cancers13112601.
38. Zhang Z, Yamashita H, Toyama T, Sugiura H, Ando Y, Mita K, et al. NCOR1 mRNA is an independent prognostic factor for breast cancer. Cancer Lett. 2006;237:123–9. https://doi.org/ 10.1016/j.canlet.2005.05.046.
39. Shu S, Li Z, Liu L, Ying X, Zhang Y, Wang T, et al. HPV16 E6-Activated OCT4 Promotes Cervical Cancer Progression by Suppressing p53 Expression via Co-Repressor NCOR1. Front Oncol. 2022;12:900856. https://doi.org/10.3389/fonc.2022.900856.
40. St-Jean S, De Castro AC, Lecours M, Jones C, Rivard N, Rodier F. NCOR1 Sustains Colorectal Cancer Cell Growth and Protects against Cellular Senescence. Cancers. 2021;13(17):4414. https://doi.org/10.3390/cancers13174414.
41. Tan J, Zhang S, Li L, Mu J, Wang Z, Zhang L, et al. Abnormally localized DLK1 interacts with NCOR1 in non-small cell lung cancer cell nuclear. Biosci Rep. 2019;39(12):BSR20192362. https://doi.org/10.1042/bsr20192362.
42. Detilleux D, Raynaud P, Pradet-Balade B, Helmlinger D. The TRRAP transcription cofactor represses interferon-stimulated genes in colorectal cancer cells. Elife. 2022;11:e69705. https://doi.org/10.7554/eLife.69705.
43. Kang KT, Kwon YW, Kim DK, Lee SI, Kim KH, Suh DS, et al. TRRAP stimulates the tumorigenic potential of ovarian cancer stem cells. BMB Rep. 2018;51:514–9. https://doi.org/10.4048/jbc.2016.19.1.61.
44. Kang KT, Shin MJ, Moon HJ, Choi KU, Suh DS. TRRAP Enhances Cancer Stem Cell Characteristics by Regulating NANOG Protein Stability in Colon Cancer Cells. International Journal of Molecular Sciences. 2023;24(7):6260. https://doi.org/10.3390/ijms24076260.
45. Kwan SY, Sheel A, Song CQ, Zhang XO, Jiang T, Dang H, et al. Depletion of TRRAP Induces p53-Independent Senescence in Liver Cancer by Down-Regulating Mitotic Genes. Hepatology. 2020;71:275–90. https://doi.org/10.1002/hep.30807.
46. Wang J, Shan M, Liu T, Shi Q, Zhong Z, Wei W, et al. Analysis of TRRAP as a Potential Molecular Marker and Therapeutic Target for Breast Cancer. J Breast Cancer 2016;19:61–7. https://doi.org/10.4048/jbc.2016.19.1.61.
47. Jiang Y, Li T. Morphine in Combination with Ketamine Improves Cervical Cancer Pain and Suppresses Immune Function via the JAK3/STAT5 Pathway. Journal of Healthcare Engineering. 2022;2022:9364365. https://doi.org/10.1155/2022/9364365.
48. Jin J, Guo Q, Xie J, Jin D, Zhu Y. Combination of MEK Inhibitor and the JAK2-STAT3 Pathway Inhibition for the Therapy of Colon Cancer. Pathol Oncol Res. 2019;25:769–75. https://doi.org/10.1007/s12253-019-00592-6.
49. Li SD, Ma M, Li H, Waluszko A, Sidorenko T, Schadt EE, et al. Cancer gene profiling in non-small cell lung cancers reveals activating mutations in JAK2 and JAK3 with therapeutic implications. Genome Med. 2017;9:89. https://doi.org/ 10.1186/s13073-017-0478-1.
50. Van Allen EM, Golay HG, Liu Y, Koyama S, Wong K, Taylor-Weiner A, et al. Long-term Benefit of PD-L1 Blockade in Lung Cancer Associated with JAK3 Activation. Cancer Immunol Res. 2015;3:855–63. https://doi.org/10.1158/2326-6066.cir-15-0024.
51. Wu T, Yu J, Wang C, Jin Y, Zheng X, Chen L, et al. Novel Potent EGFR-JAK3 Dual-Target Inhibitor that Overcomes KRAS Mutation Resistance in Colorectal Cancer. Anticancer Agents Med Chem. 2023;23(4):440–9. https://doi.org/10.2174/1871520622666220609112816.
52. Zhou C, Chen L, Chen R, Xu F, Huang Z, Huang R, et al. miR-4486 enhances cisplatin sensitivity of gastric cancer cells by restraining the JAK3/STAT3 signalling pathway. J Chemother. 2022;34:35–44. https://doi.org/ 10.1080/1120009x.2021.1936957.
53. Canale M, Andrikou K, Priano I, Cravero P, Pasini L, Urbini M. The Role of TP53 Mutations in EGFR-Mutated Non-Small-Cell Lung Cancer: Clinical Significance and Implications for Therapy. Cancers (Basel) 2022;14(5):1143. https://doi.org/10.3390/cancers14051143.
54. Chen J, Chang X, Li X, Liu J, Wang N, Wu Y, et al. The heterogeneous impact of targeted therapy on the prognosis of stage III/IV colorectal cancer patients with different subtypes of TP53 mutations. Cancer Medicine. 2023;12:21920–32. https://doi.org/10.1002/cam4.6766.
55. Liu B, Yi Z, Guan Y, Ouyang Q, Li C, Guan X, et al. Molecular landscape of TP53 mutations in breast cancer and their utility for predicting the response to HER-targeted therapy in HER2 amplification-positive and HER2 mutation-positive amplification-negative patients. Cancer Medicine. 2022;11(14):2767–78. https://doi.org/ 10.1002/cam4.4652.
56. Liu J, Gao J. Efficacy of immunotherapy as second-line or later-line therapy and prognostic significance of KRAS or TP53 mutations in advanced non-small cell lung cancer patients. Eur J Cancer Prev. 2023;32:590–9. https://doi.org/10.1097/cej.0000000000000799.
57. Michikawa C, Torres-Saavedra PA, Silver NL, Harari PM, Kies MS, Rosenthal DI, et al. Evolutionary Action Score of TP53 Analysis in Pathologically High-Risk Human Papillomavirus-Negative Head and Neck Cancer From a Phase 2 Clinical Trial: NRG Oncology Radiation Therapy Oncology Group 0234. Advances in Radiation Oncology. 2022;7(6):100989. https://doi.org/ 10.1016/j.adro.2022.100989.
58. Roeper J, Christopoulos P, Falk M, Heukamp LC, Tiemann M, Stenzinger A, et al. TP53 co-mutations as

an independent prognostic factor in 2nd and further line therapy-EGFR mutated non-small cell lung cancer IV patients treated with osimertinib. Transl Lung Cancer Res. 2022;11:4–13. https://doi.org/10.21037/tlcr-21-754.
59. Sun H, Ren P, Chen Y, Lan L, Yan Z, Yang Y, et al. Optimal therapy for concomitant EGFR and TP53 mutated non-small cell lung cancer: a real-world study. BMC Cancer. 2023;23:198. https://doi.org/ 10.1186/s12885-023-10637-4.
60. Abdelhamid D, Abdel-Aziz M, Li X, Jiang W, Dong S, Li W, et al. STAT3 Inhibitors: A Novel Insight for Anticancer Therapy of Pancreatic Cancer. Biomolecules 2022;12(10):1450. https://doi.org/10.3390/biom12101450.
61. Allam A, Yakou M, Pang L, Ernst M, Huynh J. Exploiting the STAT3 Nexus in Cancer-Associated Fibroblasts to Improve Cancer Therapy. Front Immunol. 2021;12:767939. https://doi.org/10.3389/fimmu.2021.767939.
62. Dong J, Cheng XD, Zhang WD, Qin JJ. Recent Update on Development of Small-Molecule STAT3 Inhibitors for Cancer Therapy: From Phosphorylation Inhibition to Protein Degradation. Journal of Medicinal Chemistry. 2021;64(13):8884–8915. https://doi.org/10.1021/acs.jmedchem.1c00629.

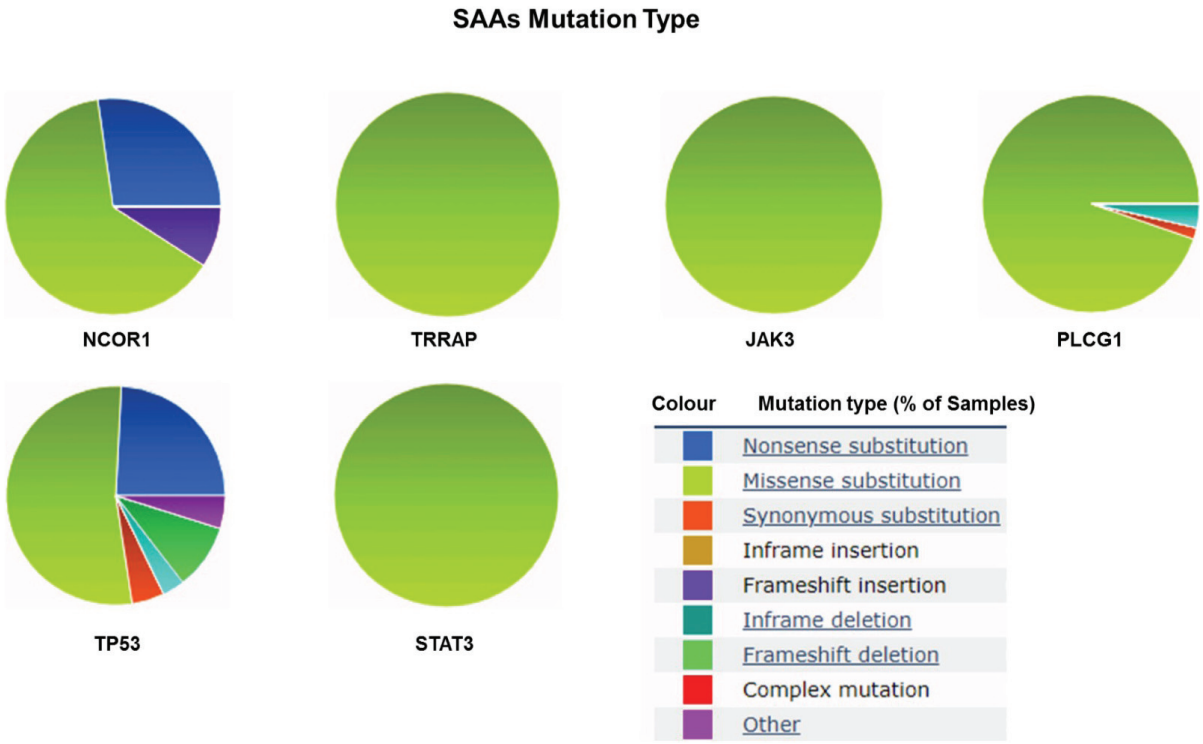

Supplementary Figure 1.